

# XANES microimaging and tomography

C. Rau<sup>a</sup>, A. Somogyi<sup>b</sup>, A. Bytchkov<sup>a</sup> and A. Simionovici<sup>a</sup>

<sup>a</sup> ESRF, 6 rue Jules Horowitz, BP 220, F-38043 Grenoble CEDEX, France

<sup>b</sup> University of Antwerp, Department of Chemistry, Universiteitsplein 1, B-2610 Wilrijk-Antwerp, Belgium

## ABSTRACT

In chemistry, X-ray absorption near-edge spectroscopy (XANES) is a well-known and established technique. By scanning the X-ray energy in the vicinity (50-100 eV) of the absorption edge of an element, information can be obtained about the oxidation state of the probed atoms. The (conventional) technique mainly employed until now applies for homogeneous, specifically prepared flat samples where the measured signal can be considered as the average over the whole irradiated volume. This restriction for samples is partially released when the XANES method is combined with imaging techniques. 2-D resolved data is acquired using area detectors or by scanning with a focussed beam. X-ray absorption tomography is a method of choice for investigating the 3D structure of objects and its dual energy version is used for getting information about the 3D distribution of a given element within the sample. Although the combination of XANES and tomography seems to be a natural extension of dual-energy tomography, in practice several experimental problems have to be overcome in order to obtain useable data. In the following we describe the results of XANES imaging and tomography obtained measuring a phantom sample of pure molybdenum compounds using a FreLoN 2000 camera system at the ESRF undulator beamline ID22. This system allowed making volume resolved distinctions between different oxidation states with spatial resolution in the micrometer range.

**Keywords:** XANES-tomography, spectroscopy, microtomography, full-field imaging, synchrotron radiation, hard X-rays

## 1. INTRODUCTION

Recently the need for micro-analysis is continuously increasing in various fields, such as chemistry, environmental science, material science, etc. Frequently 3D information is needed about the micro-morphology and chemical characteristics of the object, which is a challenging task for modern micro-analytical methods.

Tomography in general is a method dedicated to obtaining information about the 3D morphology of the sample. It is also possible to acquire detailed volume information by using some surface sensitive techniques, such as electron-probe micro-analysis, by removing layer by layer from the sample. Sometimes these methods are also called "tomography"<sup>1</sup>, despite their destructive nature. On the other hand there remain also problems such as the destruction of the fine inner structure by sectioning, the modification of the chemical structure at the surface, preferential removing of elements (in the case of ion bombardment for SIMS), or precipitation of dissolved elements on the surface (like it can happen e.g. etching silver containing glasses). The destruction or modification of the structure by the treatment cannot be excluded as a matter of principle. Also chemical bonding is changing near or at the surface. In general it remains an open question if the structure observed at the surface corresponds to that inside the volume.

Another way to obtain detailed in-volume information is to combine non-destructive X-ray analytical methods such as X-ray absorption tomography and X-ray spectroscopy, such as fluorescence spectroscopy or XANES.

X-ray absorption tomography is an imaging technique, which gives spatially resolved 3D information about the distribution of the linear absorption coefficient of the sample, by measuring the 2D transmission images of the object at different projection angles.

XANES is a well-known and established technique to identify the oxidation state of a probed atom. It is based on the measurement of the fine structure of the elements absorption edge. By using XANES the measured signal is usually spatially integrated. As a consequence the studied material is considered to be homogeneous and is often specially prepared as flat samples.

As the same physical quantity as in X-ray tomography is measured - absorption- the idea is to combine both methods by changing consecutively the variable parameters of each, which are projection angle and energy. Tomographic scans above and below the element specific absorption edge have been done already in the past, allowing to identify the elemental distribution inside the sample<sup>2-5</sup>. Repeating tomographic scans with a fine energy grid should permit to establish a complete XANES spectrum for each voxel inside the sample. The combined usage of 2D mapping and XANES techniques (XANES-imaging) has been shown in the past<sup>6-9</sup> and opens new possibilities in obtaining micrometer-resolved 2D chemical information in X-ray analysis<sup>10-12</sup>.

## 2. EXPERIMENTAL

In a first step of the experiment we realised XANES-imaging in a full-field set-up at the ESRF undulator beamline ID22. The success of this experiment was a basic condition for the following XANES-tomography experiment. This implies for example a linear detector response and a clean and flat beam, as well as a monochromator able to deliver a fixed-exit beam as a function of the energy.

### 2.1. XANES

A classical XANES set-up is represented in figure 1. In the case of transmission XANES the intensity of the incoming monochromatic beam is measured with a detector, such as an ionisation chamber or a PIN diode. The X-rays are partially absorbed by the sample. The transmitted intensity is measured with a second detector.

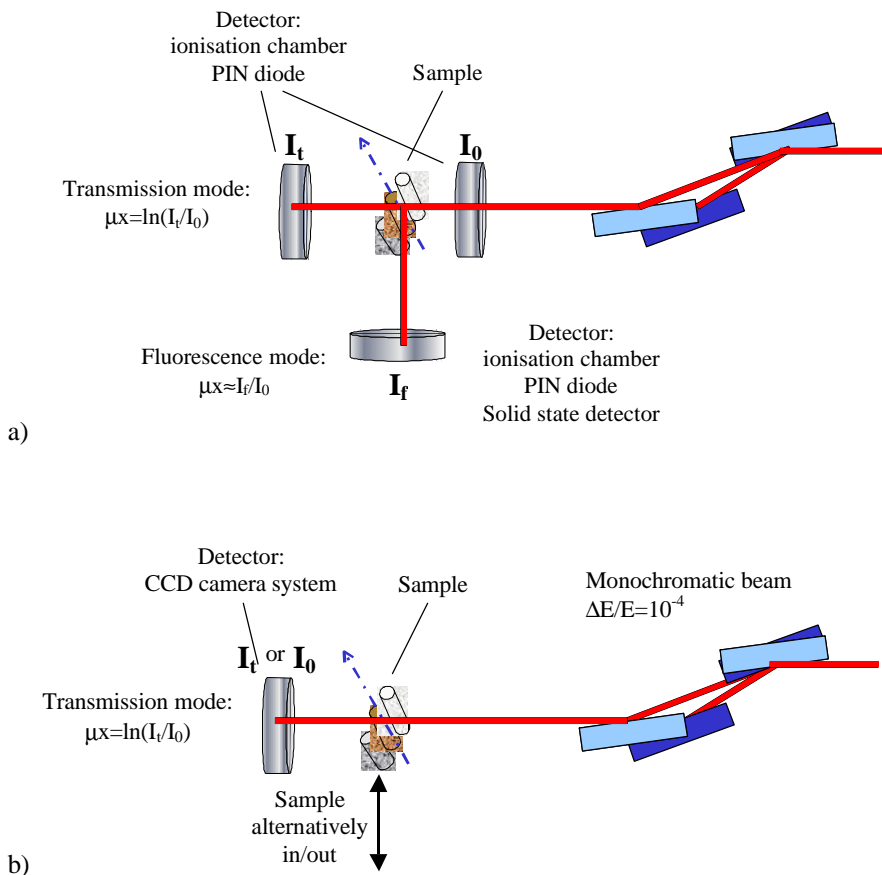


**Figure 1:** a) Set-up for XANES in transmission mode and in fluorescence mode. With a focussing lens 2-D resolved measurements are possible by scanning the sample.

b) Set-up for XANES full-field imaging. The Flat-field image corresponds to the measure  $I_0$ , the projection image to  $I_{\text{trans}}$ , using the same detector (CCD camera).

The measurement consists in scanning the energy, while registering  $I_{\text{trans}}$  and  $I_0$ . This measurement can be repeated several times in order to improve the statistics. According to the Beer-Lambert law the product of the linear absorption coefficient  $\mu(E)$  and the thickness  $x$  of the irradiated pixel of the sample can be deduced as a function of the  $E$  energy from the relation  $\mu(E)x = \ln(I_0/I_{\text{trans}})$ .

Since  $\ln(I_0/I_{\text{trans}})$  depends on the thickness of the irradiated area of the sample, any inhomogeneity such as holes, thickness or concentration variation can lead to artefacts which will distort the spectrum in case of measuring the average XANES spectrum at a given zone of a sample considered to be homogeneous. Thus in most cases the samples are specially prepared by grinding, sieving and eventually diluting the powder in boron nitride for pressing finally homogeneous pellets with ideal thickness. Usually the 'ideal' thickness of the sample is chosen in such a way that the  $\ln(I_{\text{trans,below}}/I_{\text{trans,above}})$  absorption jump at the absorption edge is about -1, where  $I_{\text{trans,below}}$  is the transmitted before the absorption edge and  $I_{\text{trans,above}}$  after the absorption edge respectively.

In the case of very low concentrations of the studied element or very thin samples alternatively, the absorption of the incoming radiation due to the probed element is very small, thus usually the intensity of its characteristic X-ray fluorescence signal is registered. Since the fluorescence mode cannot be combined with a full-field imaging technique, this method will not be discussed in detail here.

## 2.2 XANES-imaging and tomography

In order to get bi-dimensionally resolved XANES information two different solutions are possible. The first one consists in a scanning technique with focussed beam either in transmission or fluorescence mode<sup>6,7</sup> and the second by using a 2D area detector in transmission mode. The inconvenience of the first technique is that a measurement is rather time-consuming. The sample has to be scanned over the surface point by point and efficiency of x-ray lenses used for beam focussing is low (e.g. for parabolic CRLs:  $T < 5\%$ ).

The XANES-imaging and tomography experiments, were performed in a full-field technique at the ESRF end-station ID22<sup>13-15</sup>. The experimental set-up consisted of the following components:

The X-ray beam is generated by an undulator at the high-beta section of the electron storage ring of the ESRF. The source size is about 800  $\mu\text{m}$  horizontal x 30  $\mu\text{m}$  vertical (FWHM)<sup>16</sup>. The energy of the beam is defined by a KHOZU fixed-exit monochromator. With a set of two Si (111) crystals the bandwidth  $\Delta E/E$  is  $10^{-4}$ . In order to suppress the higher harmonics, which might pass the monochromator, an X-ray mirror is placed between the undulator and monochromator, which reduces also the heat load of the intense beam on the monochromator. The flat mirror is a silicon single crystal with a total length of 90 cm. The surface roughness is about 1.5  $\text{\AA}$  (RMS). The different coating strips on the mirror and the deflection angle define the cut-off energy. The platinum-strip was chosen in combination with an incident angle of 0.15 degree for the experiments, defining a cut-off energy of about 32 keV.

The imaging and tomography set-up is placed at about 65 m distance from the source in the second hutch. In order to reduce the optical elements in the beam such as beryllium windows at the entrance of vacuum sections and to diminish air absorption at low energies the first experimental hutch is bridged with a vacuum tube. All optical elements in the beam like beryllium windows, monochromator and mirror were selected for their high optical quality in order to have a homogeneous, flat and artefact-free "clean" beam.

The x-rays are measured by a CCD camera system, coupled to a microscope and scintillation screen. The camera is an in-house developed FreLoN 2000 CCD camera<sup>17</sup>. The low read out noise and the high dynamic range of 14 bit makes this system to an ideal device for the requested task. The scintillation screen consists of a Lutetium Aluminum Garnet (LAG) single crystal with a 26  $\mu\text{m}$ -thick active Europium doped layer. The effective pixel size, given by the CCD pixel size, the binning factor of the CCD pixels and the microscope magnification, is 1.4  $\mu\text{m}$ . The spatial resolution of this configuration, limited by the point spread function of the scintillation screen, is estimated to be 2-3 micron. A detailed description of the camera system can be found elsewhere<sup>13,17,18</sup>.

For both -imaging and tomography- experiments the same sample stage was used (see also<sup>14,15</sup>). The rotation axis of the tomography stage was vertical and the distance between sample and detector was minimized, because the phase contrast effects would distort the absorption spectra due to the highly coherent source.

The incoming and transmitted intensity was measured by removing (flat field image) and re-inserting the sample in the beam (projection). The reproducibility of the translation stage position is about one micron. The images were further corrected by subtracting the dark-field image.

Different molybdenum compounds were chosen for the measurements. The powders with a grain size between 2 and 50 micron were inserted in separate glass capillaries. Several of them were attached together for the imaging experiments, so that all spectra could be taken simultaneously. For the XANES tomography experiments a variable number of single capillaries were put inside a capillary with a bigger diameter. The energy of the molybdenum K-edge is at 20 keV. For the XANES-imaging experiments the energy step width used was 2 eV and the exposure time 2 sec. per image. The total time for a complete scan was about 20 minutes. Several XANES-tomography experiments were carried out with a different number of capillaries, with up to 1250 projections per half-turn for a tomographic scan and an energy step between the tomographic scans of down to 2 eV. During a tomographic scan intermediate flat-field images were taken. After each tomographic scan, the energy was changed for the next tomographic scan. For simplicity, we will present the results obtained with a sample containing only two different molybdenum powders. One capillary was filled with molybdenum oxide ( $\text{MoO}_3$ ; Aldrich, >99% purity) having a grain size between 10 and 20 microns and the other with molybdenum silicate ( $\text{MoSi}_2$ ; Goodfellow, 99,5% purity) with 45-micron grains. Additional XANES-imaging experiments we carried out with flat homogeneous samples will be reported in future.

### 3. RESULTS

#### 3.1. XANES-imaging

The different XANES-imaging spectra and some reference spectra found in literature<sup>19,20</sup> are shown in Fig. 2. The stack of images measured at different energies was aligned before evaluating the spatially resolved XANES spectra in order to correct for the possible sample movement during the measurement. The maximum misalignment found between two images was about 2 pixels, verifying the high stability of the experimental set-up during the measurements. The XANES spectra were obtained from the images by averaging the spectra of several pixels of each capillary. It is clear from comparing the two figures that the average XANES spectra of the different capillaries can be clearly identified despite of the topological effects and worse counting statistics. On the other hand the spectra of individual pixels especially around the edge of the individual grains may be too distorted to be recognisable, reflecting a thickness change on the pixel scale.

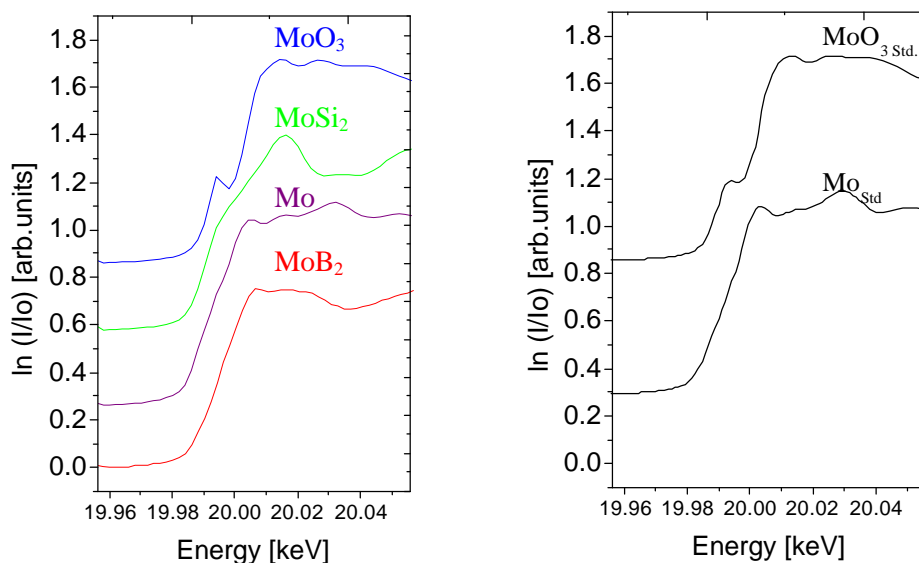


**Figure 2:** XANES spectra obtained with full-field imaging technique from powder filed capillaries (left) and spectra of standard samples found in literature<sup>19,20</sup>.

### 3.2. XANES -tomography

The XANES tomography data were evaluated for tomographic scans, taken at characteristic energies (see figure 3) obtained from the XANES imaging experiments. Each scan was reconstructed with simple filtered back projection<sup>21,22</sup>, without applying special data filtering. The XANES image of a chosen 2D slice can be obtained by creating image stacks of the reconstructed slices measured at different energies. The alignment of image stacks was done manually. The maximum misalignment found within the full image-stack was of two pixels.

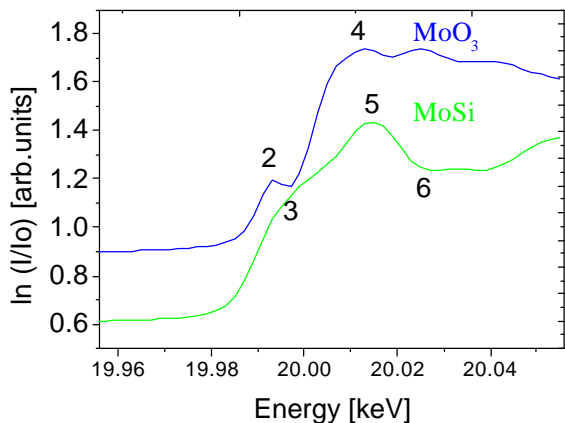


**Figure3:** Characteristic energies chosen for reconstructed data to build images of difference slices (see also figure 4).

The images of a given slice measured at different characteristic energies were subtracted from each other. The results are shown in figure 4. One can clearly see that by subtracting the reconstructed slice obtained at the energy corresponding in the scheme to "5" from energy number "6" leads to a strong contrast image for the MoSi<sub>2</sub> component while the MoO<sub>3</sub> containing capillary is not visible indicating a weak difference in absorption. This result is in perfect agreement with the variation of the absorption known from the XANES imaging experiments.

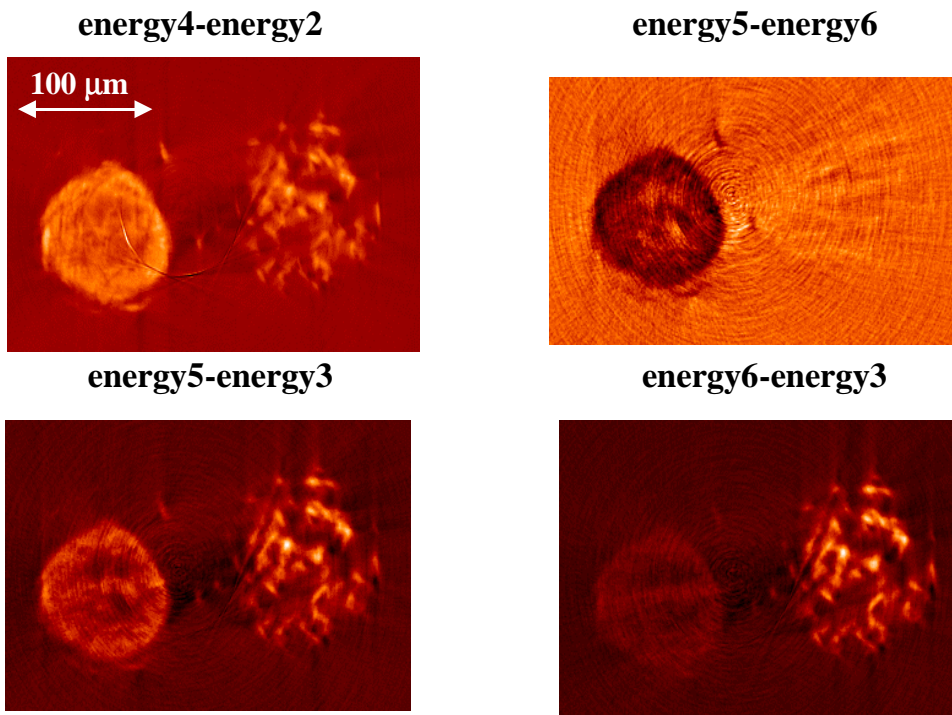


**Figure 4:** Difference slices obtained from reconstructed data taken at characteristic energies (see figure 3).

## 4. OUTLOOK AND CONCLUSION

The acquired data from the XANES-tomography experiments can be evaluated in more detail, including all available data and improvements of data reconstruction. This will lead to a complete XANES spectrum for each single voxel. This means that a sample can be segmented in different zones with a certain oxidation state by comparing the spectrum of the voxel with different possible standard spectra. This will open the field of a new in-volume chemistry allowing to study spatially resolved reaction mechanisms and other aspects for samples containing the element to be investigated in a large enough concentration.

A non-negligible part of the work in the future will concern the data analysis part as e.g. automatic alignment of images and affined data reconstruction.

It was shown for the first time, that different oxidation states can be clearly spatially identified in 3D with a resolution on the micrometer scale. This is certainly due to the high quality of the beam and detector system and the fact that the right experimental conditions were found to have almost artefact-free reconstructed data.

The advantages of this technique are obvious:

It is a non-destructive method, giving access to information not available with any other technique giving an in-depth look into chemistry inside the bulk routinely not accessible.

## ACKNOWLEDGEMENTS

Thanks to the members of the ID22 group, especially to A. Homs, J. M. Rigal, A. Snigirev and T. Weitkamp, who contributed each in their way to the success of the experiment.

## REFERENCES

- <sup>1</sup>R. Magerle, "Nanotomography", *Phys. Rev. Lett.* **85** (13), pp. 2749-2752, 2000.
- <sup>2</sup>U. Bonse, Q. C. Johnson, M. C. Nichols, R. Nusshardt, S. Krasnicke, and J. H. Kinney, "High resolution tomography with chemical specificity", *NIM A* **246**, pp. 644-648, 1986.
- <sup>3</sup>U. Bonse, R. Nusshardt, F. Buschet, R. Pahl, Q. C. Johnson, J. H. Kinney, R.A. Saroyan, and M. C. Nichols, "Optimization of CCD-based energy-modulated x-ray microtomography", *Rev. Sci. Instr.* **60** ((7)), pp. 2478-2481, 1989.
- <sup>4</sup>K. Engelke, M. Lohmann, W.-D. Dix, and W. Graeff, "A System for Dual Energy Microtomography of Bones", *NIM A* **274**, pp. 380-389, 1986.
- <sup>5</sup>J. H. Kinney, Q. C. Johnson, M. C. Nichols, U. Bonse, R. A. Saroyan, R. Nusshardt, and R. Pahl, "X-ray microtomography on beamline X at SSRL", *Rev. Sci. Instrum.* **60** (7), pp. 2471-2474, 1989.
- <sup>6</sup>S.R. Sutton, S. Bajt, J. Delaney, D. Schulze, and T. Tokunaga, "Synchrotron x-ray fluorescence microprobe: Quantification and mapping of mixed valence state samples using micro-XANES", *Rev. Sci. Instrum.* **66** (2), pp. 1464-1467, 1995.
- <sup>7</sup>S. Bajt, S.R. Sutton, and J. Delaney, "X-ray microprobe analysis of iron oxidation states in silicates and oxides using X-ray absorption near edge structure", *Geochimica et Cosmochimica Acta* **58** (23), pp. 5209-5214, 1994.
- <sup>8</sup>M. Bonnin-Mosbah, J. P. Duraud, N. Métrich, Z. Wu, J. S. Delaney, and A. San Miguel, "Micro-XANES with synchrotron radiation: a complementary tool of micro-PIXE and micro-SXRF for the determination of oxidation state of elements. Application to geological materials", *NIM B* **158**, pp. 214-220, 1999.
- <sup>9</sup>B. Salbu, K. Janssens, T. Krekling, A. Simionovici, M. Drakopoulos, C. Raven, I. Snigireva, A. Snigirev, O. C. Lind, and D. H. Oughton, "μ-X-ray Absorption tomography and μ-XANES for Characterisation of Fuel Particles", *ESRF Highlights*, pp. 24-25, 1999.
- <sup>10</sup>M. Bonnin-Mosbah, A. Simionovici, N. Métrich, J. P. Duraud, D. Massare, and P. Dillmann, "Iron oxidation states in silicate glass inclusions with a XANES microprobe", *Journ. Non-Cryst. Phys.* (accepted), 2001.
- <sup>11</sup>N. Métrich, M. Bonnin-Mosbah, J. Susini, and M. Salomé, "Sulfur and iron K-edges in olivine hosted glass inclusions by micro-XANES", *Geographical Research Letter*, submitted.
- <sup>12</sup>M. Salomé, Y. Dauphin, J. Susini, J. Doucet, B. Fayard, and J.P. Cuif, "The role of sulfur in biomineralization explored by X-ray absorption spectroscopy with sub-micron resolution: the relationship between sulfur chemical states and shell micro-architecture in *Pinna Nobilis*", *Proc. Natl. Acad. Sci. USA (PNAS)*, submitted.
- <sup>13</sup>C. Raven, A. Snigirev, A. Koch, I. Snigireva, and V. Kohn, "X-ray tomography with micrometer spatial resolution", *SPIE Proc.* **3149**, pp. 140-148, 1997.

- <sup>14</sup>C. Raven, *Microimaging and Tomography with High-Energy Coherent Synchrotron X-rays*, Shaker Verlag, Aachen, 1998.
- <sup>15</sup>T. Weitkamp, C. Raven, and A. Snigirev, "Imaging and microtomography facility at the ESRF beamline ID 22", in *Developments in X-ray Tomography II*, U. Bonse ed., SPIE proc. **3772**, pp. 311-317, 1999.
- <sup>16</sup>P. Elleaume, website <http://www.esrf.fr/machine/support/ids/Public/Sizes/sizes.html>.
- <sup>17</sup>J.-C. Labiche, J. Segura Puchades, D. v. Brussel, and J. Moy, *ESRF Newsletter* **25**, pp. 41-43, 1996.
- <sup>18</sup>A. Koch, C. Raven, P. Spanne, and A. Snigirev, "X-ray imaging with submicrometer resolution employing transparent luminescent screens", *J. Opt. Soc. Am.* **15**, pp. 1940-1951, 1998.
- <sup>19</sup>Lytle, software "website [http://ixs.iit.edu/database/data/Farrel\\_lytle\\_data/index.html](http://ixs.iit.edu/database/data/Farrel_lytle_data/index.html)".
- <sup>20</sup>M Sanchez del Rio and R.J Dejus, "XOP: recent developments", SPIE Proc. **3448**, pp. 340-345, 1998.
- <sup>21</sup>A. Hammersley, software "High-speed tomography (HST)", 2000.
- <sup>22</sup>A.C. Kak and M. Slaney, *Principles of Computerized Tomographic Imaging*, IEEE press, New York, 1988.